Optimizing the Energy Efficiency of SIMO Receivers with Compact Uniform Linear Arrays

Qing Bai, Amine Mezghani, Michel T. Ivrlač, and Josef A. Nossek
Institute for Circuit Theory and Signal Processing
Technische Universität München, Munich, Germany
Email: bai@tum.de

***Abstract*—The energy efficiency of a multi-antenna receiver is influenced by the configuration of the antenna array it employs, *e.g.* with more receive antennas, larger capacity can be obtained while power dissipation is expected to increase. When compact uniform linear arrays are considered, the distance between adjacent antennas becomes a critical parameter due to its close relation to both spatial correlation and antenna mutual coupling, which are the major effects introduced by compact antenna arrays. In this paper, we formulate the optimization of energy efficiency with respect to both the antenna spacing and the number of antennas, and perform extensive numerical experiments to evaluate the gain that can be achieved by applying the optimization results. Moreover, we demonstrate the effects of various system parameters on the optimal antenna spacing, including mean angle of arrival, angle spread, average channel gain, and antenna loss factor, and propose also a simple approximation method to greatly reduce the complexity in finding the optimal spacing.**

I. Introduction

As one of the major techniques to meet the ever-increasing demand in spectral efficiency, the employment of multiple antennas at radio transmitters and/or receivers promises larger channel capacity than single antenna systems by exploiting the spatial diversity. There are also a number of limiting factors of multi-antenna systems. The associated high hardware complexity and power dissipation necessitate careful design to improve the energy efficiency of these systems. On the other hand, physical restriction on the size of communication devices limits the maximal number of antennas that can be deployed, the problem of which can be approached by using *compact antenna arrays*. Conventionally, the spacing between adjacent antennas is taken as half of the wavelength, which satisfactorily reduces the effects of mutual coupling between antennas. Moving the antennas still closer leads to pronounced spatial correlation [1] and strong mutual coupling [2], the effects of which on the channel capacity have been thoroughly investigated. Applying circuit theory to communications, the authors of [3] developed a linear multiport model for multi-antenna systems which is in consistency with the underlying physics. The model has been adopted by other works such as [4] for investigations of various communication systems with compact antenna arrays.

The introduction of spatial correlation to receiver noise by antenna mutual coupling and the impedance matching network is explained in [3], which further gives closed form expressions for the noise covariance matrix as a function of the antenna spacing for isotropic radiators. The paper showed the potential of exploiting the coupling effects with signal processing, by demonstrating the enhancement of transmit and receive array gains with antenna spacing well below half of the wavelength. In this paper, we consider a multi-antenna receiver with a compact antenna array and focus on the optimization of energy efficiency of the system with respect to the array parameters, including antenna spacing and the number of antennas. Such a formulation addresses the issues of both power consumption and space requirement associated with multi-antenna systems, and has not been explored yet to the best of our knowledge. In particular, we attempt to get insight on the dependency of the optimal antenna spacing on the number of antennas in the array, as well as the dependency of both on channel and background radiation conditions likewise antenna loss factors.

II. System Model

We consider a single-input multiple-output (SIMO) system with M isotropic receive antennas which are deployed as a uniform linear array (ULA), *i.e.*, the antennas are located on a straight line with uniform spacing in between. With the spatial correlation induced by propagation taken into account and the assumption of a Rayleigh flat-fading channel, the received signal can be modeled as

$$\boldsymbol{y} = \sqrt{\alpha}\boldsymbol{R}^{1/2}\boldsymbol{h}x + \boldsymbol{n}, \tag{1}$$

where $x \in \mathbb{C}$ is the transmitted symbol with $\mathrm{E}\left[|x|^2\right] = 1$, the positive scalar α stands for the average combined power gain of the transmit power and the wireless channel, $\boldsymbol{h} \in \mathbb{C}^M$ denotes the channel vector which contains i.i.d. Gaussian distributed entries with zero mean and unit variance, and $\boldsymbol{n} \in \mathbb{C}^M$ represents the additive noise in the receive signal. We explain next in more detail how the correlation matrix $\boldsymbol{R}$ and the covariance matrix of the noise vector are obtained.

A. Spatial correlation model of the ULA

Spatial correlation in the received signals of a multi-antenna system is introduced by sparse scattering in the propagation environment, and can be more pronounced when the separation of the receive antennas is not large enough. The modeling of the spatial correlation in MIMO systems has been well studied, *e.g.* [5]. However, most of these works restrict the multipath components arriving at the antenna array to be on the same plane in which the array also lies. This requires only a 2D modeling of the geometric relation between the signal paths and the antenna array, but overlooks the fact that the scatterers and reflectors on the way of propagation posses both different azimuths and elevations. We derive in the following a more general spatial correlation model which allows one more degree of freedom in the angles of signal arrivals.

978-1-4799-5863-4/14/$31.00

Let us enumerate the antenna elements of the ULA sequentially by integer numbers $0, 1, \ldots, M-1$, and take antenna 0 as the reference antenna. We set up a 3D coordinate frame where this antenna is located in the origin, as shown in Figure 1. Suppose the receive signal arrives with a group of signal paths where the central arriving direction is in parallel with the z-axis. We define the *angle of arrival* (AOA) as the angle between the ULA-axis and the direction from which the wavefront is impinging on the antenna array. With this definition, the *end-fire* direction refers to the AOA of 0 degree, whereas the *front-fire* direction refers to the AOA of 90 degrees. Let the average AOA be denoted with θ_0, *i.e.* the angle between the ULA-axis and the z-axis is θ_0. Furthermore, we restrict the ULA-axis to lie in the y-z plane so that the coordinate system is fully determined. Consider that the maximal AOA deviation from θ_0 is $\Delta\theta$, and that the angle between the potential signal paths and the z-axis, denoted with θ, is continuously distributed on $[0, \Delta\theta]$. On the other hand, the angle between the x-axis and the projection of the signal path to the x-y plane, denoted with ϕ, is continuously distributed on $[0, 2\pi]$. In Figure 1, we illustrate one signal path with the straight red line. Let A be a point on that line with distance r to the origin, and let point D indicate the location of antenna 1. The coordinates of the two points are given by

$$A\left(r\sin\theta\cos\phi, r\sin\theta\sin\phi, r\cos\theta\right),\ D\left(0, d\sin\theta_0, d\cos\theta_0\right),$$

where d is the uniform antenna spacing. The corresponding AOA of the signal path, denoted with φ, can be obtained via

$$\cos\varphi = \sin\theta\sin\phi\sin\theta_0 + \cos\theta\cos\theta_0,$$

from which we can directly compute the array steering vector

$$\boldsymbol{a}(\theta,\phi) = \left[\begin{array}{cccc} 1 & \mathrm{e}^{-\mathrm{j}kd\cos\varphi} & \cdots & \mathrm{e}^{-\mathrm{j}(M-1)kd\cos\varphi} \end{array}\right]^{\mathrm{T}},$$

where constant $k = 2\pi/\lambda$ and λ denotes the wavelength of the signal. Assuming the signals impinge with uniform power density (constant power per area), the spatial correlation feature of the antenna array is captured by the matrix

$$\boldsymbol{R} = \xi \int_{\phi=0}^{2\pi}\int_{\theta=0}^{\Delta\theta} \sin\theta\cdot\boldsymbol{a}(\theta,\phi)\boldsymbol{a}^{\mathrm{H}}(\theta,\phi)\,\mathrm{d}\theta\mathrm{d}\phi,$$

where the constant scalar $\xi \in \mathbb{R}^{+}$ normalizes the diagonal elements of the matrix to unity. Note that the positive semi-definite matrix $\boldsymbol{R}$ depends on the antenna spacing d and the mean AOA θ_0 via the array steering vector $\boldsymbol{a}$, and is also dependent on the angle spread of the multipath components indicated by $2\Delta\theta$. The matrix $\boldsymbol{R}^{1/2}$ as in (1) is a matrix square root of $\boldsymbol{R}$, that is, it satisfies $\boldsymbol{R} = \boldsymbol{R}^{1/2}\boldsymbol{R}^{1/2,\mathrm{H}}$.

B. Noise correlation

Antennas respond to the total electromagnetic field which consists of the superposition of the incident field and the field which is caused by the antennas themselves by their acting as scatterers. This scattered field of the antennas manifests as mutual coupling between their excitation ports. Various works have investigated the effects of antenna coupling on received signal component *e.g.* [6] as well as on noise *e.g.* [7]. It was pointed out in [3] that both *intrinsic* and *extrinsic* noise of the receiver are affected by antenna coupling, where the former refers to the noise caused by the low noise amplifier (LNA) and subsequent circuit components, and the latter originates from the background radiation picked up by the array of antennas. Furthermore, [3] gives analytical expressions of an impedance matching network at the receiver side which is capable of decoupling the antennas. In the special case of ULA and isotropic background radiation, the covariance matrix of the noise vector $\boldsymbol{n}$ in model (1) can be given analytically by

$$\boldsymbol{R}_{nn} = \mathrm{E}\left[\boldsymbol{n}\boldsymbol{n}^{\mathrm{H}}\right] = \sigma^2\left(\boldsymbol{C} + \gamma\cdot\boldsymbol{1}_M\right),$$

where the matrix $\boldsymbol{C}$, computed as

$$\boldsymbol{C} = \left[\begin{array}{ccccc} 1 & j_0(kd) & j_0(2kd) & j_0(3kd) & \cdots \\ j_0(kd) & 1 & j_0(kd) & j_0(2kd) & \ddots \\ \vdots & \ddots & \ddots & \ddots & \ddots \end{array}\right] \in \mathbb{R}^{M\times M}$$

with $j_0(x) = \dfrac{\sin x}{x}$, results from the mutual coupling between antennas, and the term $\gamma\cdot\boldsymbol{1}_M$ accounts for the heat loss of the antennas with γ being the constant loss factor *i.e.*, the ratio of the effective loss resistance and the radiation resistance of the antennas. The parameter σ^2 denotes the noise power per antenna when the antennas are lossless, *i.e.*, $\gamma = 0$. We make the assumption of isotropic background noise mainly for better tractability of the problem, yet it can be justified for many scenarios *e.g.* with receivers employing well designed LNA or operating in an environment with substantial interference. It can be shown that the matrix $\boldsymbol{C}$ is real-valued, Toeplitz, and positive definite for real-valued $d \neq 0$. With spacing $d \in \frac{\lambda}{2}\mathbb{N}$, we have $\boldsymbol{C} = \boldsymbol{1}_M$, which means that mutual antenna coupling does not introduce noise correlation when the antenna spacing is integer multiples of half of the wavelength. For all other spacings, the off-diagonal entries of $\boldsymbol{C}$ are nonzero.

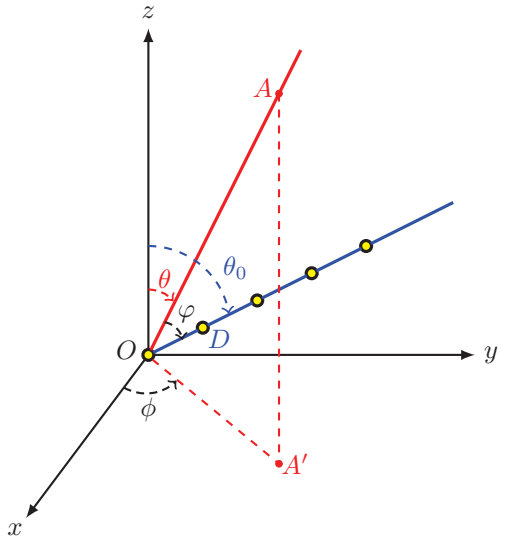

Figure 1. Obtaining a 3D spatial correlation model for a ULA of isotrops

C. Ergodic capacity and power consumption

Suppose the receive signal $\boldsymbol{y}$ is passed through a linear filter with coefficients $\boldsymbol{w} \in \mathbb{C}^M$. The signal-to-noise ratio (SNR) at the filter output is computed as

$$\mathrm{SNR}(\boldsymbol{w}) = \frac{\alpha}{\sigma^2}\cdot\frac{\boldsymbol{w}^{\mathrm{H}}\boldsymbol{R}^{1/2}\boldsymbol{h}\boldsymbol{h}^{\mathrm{H}}\boldsymbol{R}^{1/2,\mathrm{H}}\boldsymbol{w}}{\boldsymbol{w}^{\mathrm{H}}(\boldsymbol{C}+\gamma\cdot\boldsymbol{1}_M)\boldsymbol{w}},$$

given that the receiver has perfect knowledge of $\boldsymbol{h}$. Optimizing the filter coefficients results in the maximum SNR of

$$\mathrm{SNR}_{\max} = \frac{\alpha}{\sigma^2} \cdot \boldsymbol{h}^{\mathrm{H}} \boldsymbol{R}^{1/2,\mathrm{H}} \left(\boldsymbol{C} + \gamma \cdot \mathbf{1}_M\right)^{-1} \boldsymbol{R}^{1/2} \boldsymbol{h}.$$

The ergodic channel capacity in bit/sec/Hz when the optimization of the filter coefficients is adaptively employed by the receiver is therefore given by

$$C = \mathrm{E}\left[\log_2\left(1 + \frac{\alpha}{\sigma^2} \cdot \boldsymbol{h}^{\mathrm{H}} \boldsymbol{R}^{1/2,\mathrm{H}} \left(\boldsymbol{C} + \gamma \cdot \mathbf{1}_M\right)^{-1} \boldsymbol{R}^{1/2} \boldsymbol{h}\right)\right].$$

The dependency of C on the antenna spacing d lies both in the spatial correlation matrix $\boldsymbol{R}$ and the mutual coupling matrix $\boldsymbol{C}$. It should also be noted that C is likewise a function of the distance d and the number M of receive antennas.

Power is dissipated in the receiver by its RF chains as well as baseband processing units. The main power-consuming components of the RF chain include the LNA, the analog-to-digital converter (ADC) and the frequency synthesizer [8]. Part of this power consumption is related to the data rate that can be achieved, for example, the power consumption of the ADC depends exponentially on its resolution [9]. For the baseband processing, decoding is known to be the dominant power-consuming module [10], which is yet much influenced by technical details such as the specific decoding scheme and the number of iterations. For simplicity, we model the power consumption of the receiver as

$$P = M \cdot c_0 + c_1, \tag{2}$$

where the power consumption of one RF chain and the circuit power of other processing units of the receiver are represented by constants c_0 and c_1, respectively. Although the dependency on data rate is not reflected, (2) can be regarded as an average power consumption model which is suitable for our optimization problem on the static system parameters d and M. For simulations we have taken $c_0 = 10$ mW, $c_1 = 50$ mW.

III. Maximization of Energy Efficiency

The ratio between channel capacity or achievable data rate and the power consumption of the system, which gives the number of bits conveyed per consumed Joule of energy, is a common and straightforward figure of merit to measure the energy efficiency of communication systems. With the ergodic capacity and power consumption formulas derived in the last section, we formulate the energy efficiency maximization problem with respect to the number of receive antennas M and the uniform antenna spacing d of the ULA as

$$\max_{M,d} \quad \frac{C(M,d)}{P(M)} \triangleq \eta(M,d), \tag{3}$$

where η has the unit bit/Joule/Hz. A practical constraint that might be necessary to add to (3) is an upper limit on the geometric aperture of the array given by $(M-1)d$. In this work we focus on the unconstrained problem, and interestingly, we will see that the optimal antenna spacing d^* and the optimal number of antennas M^* that gives the maximal energy efficiency η^*, lead in fact to a rather small array size.

We restrict the optimization variables M to be a positive integer and d a positive real number. A straightforward way to solve (3) is to first optimize d by using line search with fixed M, and then enumerate M to look for peaks in the function η. It turns out the search space for this procedure is quite moderate, since we do not need very high precision of d^* (a searching step size of 0.01λ is used in the simulations), and the optimal antenna number M^* is also not extremely large.

IV. Numerical Results and Analysis

For numerical studies on the solutions of (3), we compute the ergodic capacity C by averaging over 2×10^5 randomly generated channel realizations. The carrier frequency does not influence the optimization results given that the antenna spacing d is expressed in terms of the wavelength λ.

A. Optimal antenna spacing with given antenna number

Noting that the power consumption P does not depend on d, we find that with fixed number of antennas, the optimal antenna spacing d^* is in fact the capacity maximizer. Figure 2 shows the variation in C with respect to d in both end-fire and front-fire directions, and with several chosen values of γ and $\Delta\theta$, when the antenna number is fixed to 4. Oscillations can be expected due to the sinc function that appears in elements of the coupling matrix $\boldsymbol{C}$. Obviously, the system behaves very differently in the front-fire and the end-fire directions. In the end-fire scenario, the optimal spacing approaches 0 if the antennas are lossless, and an optimal spacing below $\lambda/2$ can be found when the antenna loss is small. It is also worth noting that the optimal spacing increases with more antenna loss. However, in Figure 2(c), we see that it takes a rather large antenna spacing before the capacity curves settle down to oscillate around a stable average capacity. It can be further observed that with larger angle spread, this *coherence spacing* decreases. This effect is due to the better ability of the antenna array to obtain diversity when d increases. With rather lossy antennas, the stable capacity value that the curves converge to can be larger than the capacity achieved at the first peak, leading to an undesirable situation $d^* \gg \lambda/2$. Fortunately, after a closer inspection, we find that the difference in the achieved capacity at the coherence spacing and at the first peak is rather small given γ not extremely high. Therefore, in the end-fire direction, we can restrict the search for d^* within $\lambda/2$, as it does not make sense to use a very large antenna spacing that gives rather limited gain in capacity. The optimal antenna spacing in some of the test scenarios are listed in Table I.

In the front-fire direction on the other hand, the optimal spacing is generally between $\lambda/2$ and λ, and is not sensitive to antenna loss. With small to medium loss of the antennas, the maximal capacity achieved in the front-fire direction is typically less than that of the end-fire direction, especially when the angular spread is small. In the following, we focus on the scenario where the mean arriving angle of the receive signal is in the end-fire direction due to the better performance with this configuration. Yet the robustness of using the front-fire direction against antenna loss also has the potential to be exploited in certain applications.

We further explore the dependencies of the optimal antenna spacing on the number of antennas as well as on α/σ^2, the results of which are shown in Figure 3(a) and 3(b). It turns out that d^* is almost independent of α/σ^2, which means that the array configuration can stay optimal irrespective of changes

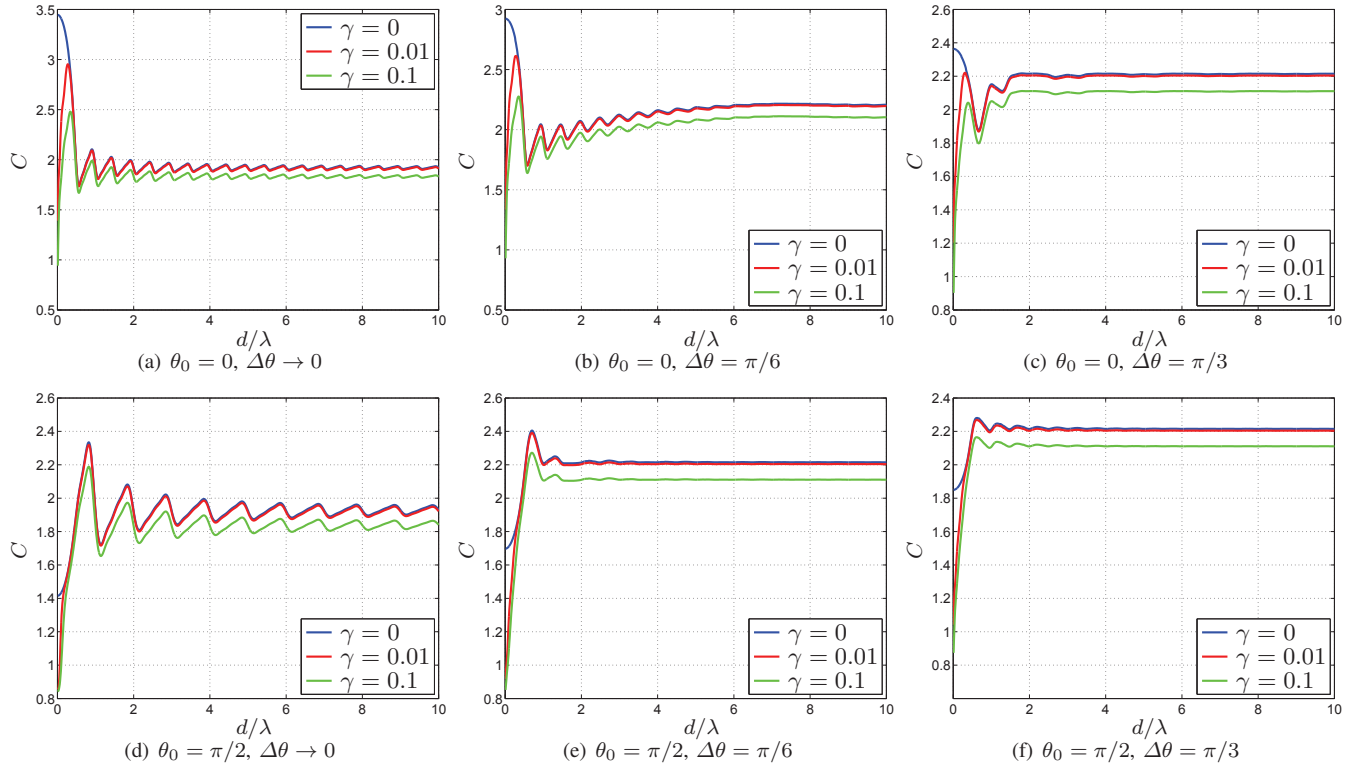

(a) $\theta_0 = 0$, $\Delta\theta \to 0$ (b) $\theta_0 = 0$, $\Delta\theta = \pi/6$ (c) $\theta_0 = 0$, $\Delta\theta = \pi/3$

(d) $\theta_0 = \pi/2$, $\Delta\theta \to 0$ (e) $\theta_0 = \pi/2$, $\Delta\theta = \pi/6$ (f) $\theta_0 = \pi/2$, $\Delta\theta = \pi/3$

Figure 2. Ergodic capacity C in bit/sec/Hz as dependent on the antenna spacing d ($M = 4$, $\alpha/\sigma^2 = 0$ dB)

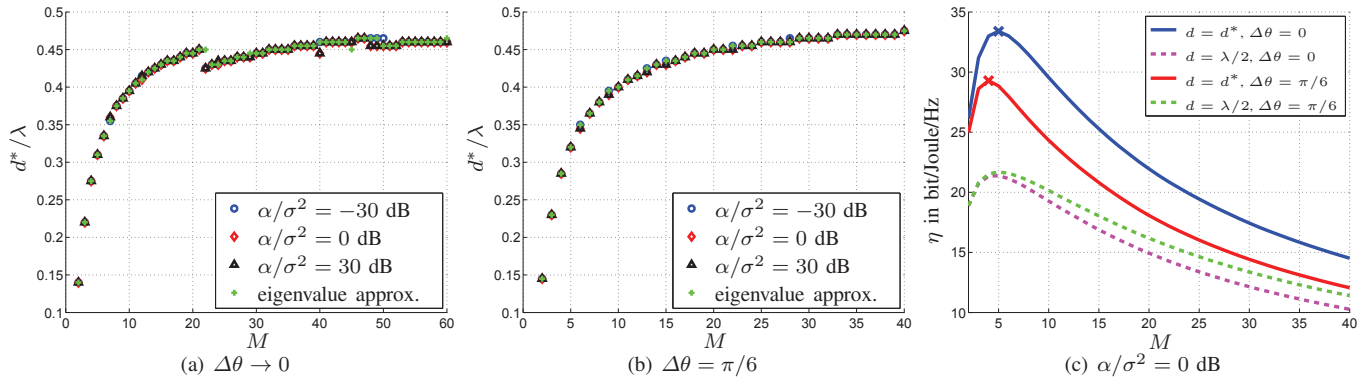

(a) $\Delta\theta \to 0$ (b) $\Delta\theta = \pi/6$ (c) $\alpha/\sigma^2 = 0$ dB

Figure 3. Dependency of optimal antenna spacing d^* and energy efficiency η on M ($\theta_0 = 0$, $\gamma = 0.01$)

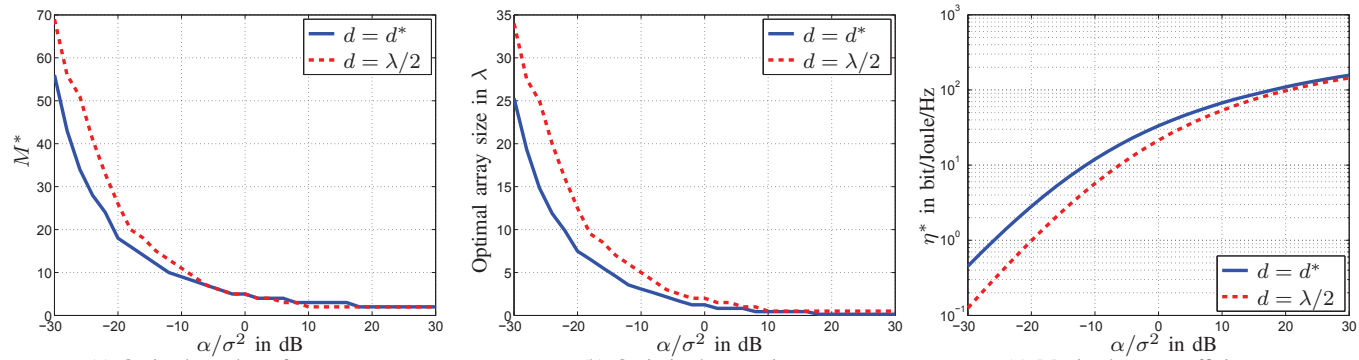

(a) Optimal number of antennas (b) Optimized array size (c) Maximal energy efficiency

Figure 4. Optimizing the energy efficiency ($\theta_0 = 0$, $\Delta\theta \to 0$, $\gamma = 0.01$)

Table I. OPTIMAL ANTENNA SPACING d^* IN FRACTIONS OF λ

	θ_0	$\Delta\theta$	$\gamma = 0$	$\gamma = 0.01$	$\gamma = 0.1$
$M = 2$	0	$\to 0$	$\to 0$	0.14	0.23
		$\pi/6$	$\to 0$	0.15	0.24
		$\pi/3$	$\to 0$	0.17	0.28
	$\pi/2$	$\to 0$	0.72	0.72	0.72
		$\pi/6$	0.71	0.71	0.71
		$\pi/3$	0.66	0.66	0.66
$M = 4$	0	$\to 0$	$\to 0$	0.27	0.34
		$\pi/6$	$\to 0$	0.28	0.35
		$\pi/3$	$\to 0$	0.31	1.82
	$\pi/2$	$\to 0$	0.82	0.82	0.82
		$\pi/6$	0.70	0.70	0.70
		$\pi/3$	0.63	0.62	0.61

in the path loss of the channel, as well as changes in the strength of the background radiation. On the other hand, it is rather surprising to observe that d^* is not exactly a monotonic function of M when $\Delta\theta \to 0$. As shown in Figure 3(a), there are a few points at which the value of d^* has a sudden decrease. This is caused by the small ripples which appear around the peaks in the capacity curves. As M varies, a small ripple could become pronounced until it surpasses the peak, thus changing d^* in a discontinuous manner. Such behavior is confirmed also with the so-called *eigenvalue approximation*. The ergodic capacity of the channel can be upper bounded, according to Jensen's inequality, by

$$\begin{aligned} C &\leq \log_2\left(1 + \frac{\alpha}{\sigma^2} \cdot \mathrm{E}\left[\boldsymbol{h}^{\mathrm{H}} \boldsymbol{R}^{1/2,\mathrm{H}} \left(\boldsymbol{C} + \gamma \cdot \mathbf{1}_M\right)^{-1} \boldsymbol{R}^{1/2} \boldsymbol{h}\right]\right) \\ &= \log_2\left(1 + \frac{\alpha}{\sigma^2} \cdot \mathrm{tr}\left(\boldsymbol{R}^{1/2,\mathrm{H}} \left(\boldsymbol{C} + \gamma \cdot \mathbf{1}_M\right)^{-1} \boldsymbol{R}^{1/2}\right)\right) \\ &= \log_2\left(1 + \frac{\alpha}{\sigma^2} \cdot \sum_{i=1}^{M} \lambda_i\right), \end{aligned}$$

where λ_i, $i = 1, \ldots, M$ denote the eigenvalues of matrix $\boldsymbol{R}^{1/2,\mathrm{H}} \left(\boldsymbol{C} + \gamma \cdot \mathbf{1}_M\right)^{-1} \boldsymbol{R}^{1/2}$. Obviously, the optimal antenna spacing that maximizes this capacity upper bound is independent of α/σ^2, and it coincides with the optimal spacing we obtain from averaging over 2×10^5 channel realizations very well (though the gap between the capacity and its upper bound is quite significant). This means, the offline search for d^* can be greatly simplified by using the eigenvalue approximation.

B. Energy efficiency maximizing array configuration

The variation of energy efficiency with respect to M when d is optimized is shown in Figure 3(c) for $\alpha/\sigma^2 = 0$ dB. There are clearly optimal values for M, which are quite small for the illustrated test scenario. The well-known trade-off between energy efficiency and spectrum efficiency [11] is seen here as for $M < M^*$, η and C can be improved at the same time by increasing M, while for $M \geq M^*$, the increment in capacity by employing more receive antennas leads to degradation of the energy efficiency of the system. The energy efficiency of the conventional usage of $d = \lambda/2$ is drawn with dashed lines for comparison. The considerable gap in η^* emphasizes the necessity of performing optimizations on d and M.

Finally, in Figure 4, we show the variation in the optimal number of antennas M^*, the optimal array size $d^*(M^* - 1)$, and the maximal energy efficiency η^* with respect to α/σ^2. With increasing α/σ^2, less antennas and less space between the antennas are required for improving the energy efficiency of the system, and the decrease in M^* and the optimal array size is close to being linear in α/σ^2. The potential of compact antenna arrays is clearly seen for a wide range of α/σ^2. Note that the specific numbers of M^* can be different if other values of the constant power consumptions c_0 and c_1 are chosen, yet the trends as shown in the figures are representative.

V. CONCLUSION

We investigate in this work the improvement of energy efficiency of a SIMO receiver which employs a compact ULA and receive linear beamforming, by optimizing the number of antennas in the array and the uniform spacing between them. To this end, a signal model that considers both spatial correlation and antenna mutual coupling is employed, and the maximization of the ratio between the ergodic channel capacity and power consumption of the receiver is formulated. From extensive numerical studies, we have learned the following: (i) Larger capacity can be achieved with received signals centered around the end-fire direction of the antenna array, while the front-fire direction exhibits better robustness against antenna heat loss; (ii) In the end-fire direction, the capacity-maximizing antenna spacing is below half of the wavelength and increases in general with growing number of antennas; (iii) The optimal antenna spacing is practically independent of the path loss of the fading channel and the strength of the noise, and can be obtained via the eigenvalue approximation; (iv) With good channel conditions and a less noisy environment, compact antenna arrays with a small number of antennas located close to each other is favorable from an energy efficiency point of view. The presented methods and results can serve as theoretical guidance for the deployment of uniform linear antenna arrays for low-power communication devices.

REFERENCES

[1] D. Shiu, G. J. Foschini, M. J. Gans and J. M. Kahn, *Fading correlation and its effect on the capacity of multielement antenna systems*, IEEE Trans. on Communications, vol. 48, pp. 502-513, March 2000.

[2] T. Svantesson and A. Ranheim, *Mutual coupling effects on the capacity of multielement antenna systems*, IEEE ICASSP'01, vol. 4, May 2001.

[3] M. T. Ivrlač and J. A. Nossek, *Toward a Circuit Theory of Communication*, IEEE Trans. on Circuits and Systems, vol. 57, no. 7, July 2010.

[4] Y. Hassan, R. Rolny and A. Wittneben, *MIMO Relaying with Compact Antenna Arrays: Coupling, Noise Correlation and Superdirectivity*, IEEE 24th PIMRC, September 2013.

[5] A. Forenza, D. J. Love and R. W. Heath, *Simplified Spatial Correlation Models for Clustered MIMO Channels With Different Array Configurations*, IEEE Trans. on Vehicular Technology, vol. 56, July 2007.

[6] J. W. Wallace and M. A. Jensen, *Mutual coupling in MIMO wireless systems: a rigorous network theory analysis*, IEEE Trans. on Wireless Communications, vol. 3, pp. 1317-1325, July 2004.

[7] C. P. Domizioli, B. L. Hughes, K. G. Gard and G. Lazzi, *Noise correlation in compact diversity receivers*, IEEE Trans. on Communications, vol. 58, pp. 1426-1436, May 2010.

[8] Y. Li, B. Bakkaloglu and C. Chakrabarti, *A System Level Energy Model and Energy-Quality Evaluation for Integrated Transceiver Front-Ends*, IEEE Trans. on VLSI Systems, vol. 15, January 2007.

[9] H. S. Lee and C. G. Sodini, *Analog-to-Digital Converters: Digitizing the Analog World*, Proceedings of the IEEE, vol. 96, no. 2, February 2008.

[10] A. Mezghani and J. A. Nossek, *Modeling and Minimization of Transceiver Power Consumption in Wireless Networks*, 2011 International ITG Workshop on Smart Antennas (WSA), February 2011.

[11] Y. Chen, S. Zhang, S. Xu, and G. Y. Li, *Fundamental tradeoffs on green wireless networks*, IEEE Communications Magazine, vol. 49, no. 6, pp. 30-37, June 2011.